Available online at www.sciencedirect.com
SCIENCE DIRECT®
Journal of Power Sources 146 (2005) 698–702
JOURNAL OF POWER SOURCES
www.elsevier.com/locate/jpowsour

Development of non-flammable lithium secondary battery with ambient-temperature molten salt electrolyte Performance of binder-free carbon-negative electrode

Koichi Ui *, Takuto Minami,
Kohei Ishikawa, Yasushi Idemoto, Nobuyuki Koura

Department of Pure and Applied Chemistry, Faculty of Science and Technology, Tokyo University of Science, 2641 Yamazaki, Noda-shi, Chiba 278-8510, Japan

Available online 24 May 2005

Abstract

The performance of a binder-free carbon-negative electrode was investigated using the LiCl-saturated $AlCl_3$–1-ethyl-3-methylimizadolium chloride (EMIC) + $SOCl_2$ melt as the electrolyte for non-flammable lithium secondary batteries. Because the glass transition point of a LiCl-saturated 60.0 mol%$AlCl_3$–40.0 mol%EMIC + 0.1 mol l^{-1} $SOCl_2$ melt was −86.2 °C, the melt could be used as the electrolyte in a low-temperature domain. The binder-free carbon electrode made by the electrophoretic deposition method was used as the negative electrode. Four kinds of carbon materials, i.e., artificial graphite, natural graphite, soft carbon, and hard carbon were evaluated as the carbon electrode. For 30 cycles, the discharge capacities of these electrodes were 296–395 mAh g^{-1} and the charge–discharge efficiencies were more than 90%. The melt can be used as the electrolyte for non-flammable lithium secondary batteries and the binder-free carbon-negative electrode operates quite effectively.

Keywords: Lithium secondary battery; Ambient-temperature molten salt; Binder-free carbon-negative electrode; Aluminum chloride-1-ethyl-3-methylimidazolium chloride melt; Electrophoretic deposition method

1. Introduction

Since an organic solvent is used for the electrolyte of lithium secondary batteries in cellular phones, etc., the safety problems, such as ignition and explosion, are a concern. The safety of a battery is more important than before due to the higher capacity or stacking of lithium secondary batteries. Because of these problems, we have investigated an ambient temperature molten salt having useful characteristics, such as low volatilty, non-flammability, and wide potential window as a lithium secondary battery electrolyte from the view point of safety [1–5].

The amount of LiCl dissolution in the $AlCl_3$–EMIC melt is dependent on the existing $Al_2Cl_7^-$ concentration [6] in a Lewis acidic melt ($AlCl_3 > 50$ mol%). Li^+ can exist in the melt according to Eq. (1) [7].

$$Al_2Cl_7^- + LiCl \rightleftarrows Li^+ + 2AlCl_4^- \quad (1)$$

We reported that the addition of Li metal to a LiCl-saturated $AlCl_3$–EMIC melt, which was prepared with excess LiCl with saturation in the $AlCl_3$–EMIC melt, $Al_2Cl_7^-$, which was the ionic species for the deposited Al, was completely removed from the melt [2]. We reported that Al foil used as the negative substrate and $LiCoO_2$, $LiNiO_2$, $LiMn_2O_4$, and crystalline V_2O_5 used as the positive material operated as full cell [1]. Fuller et al. then found that the deposition reaction of Al did not happen and the nearly reversible deposition/dissolution behavior of Li was enabled by adding $SOCl_2$ [8]. We examined whether the melt could be used as an electrolyte for lithium secondary batteries. It was found that the reversible deposition/dissolution behavior of Li was possible using an

* Corresponding author. Tel.: +81 4 7124 1501x5522; fax: +81 4 7123 9890.
E-mail address: kui@rs.noda.tus.ac.jp (K. Ui).

0378-7753/$ – see front matter © 2005 Elsevier B.V. All rights reserved.
doi:10.1016/j.jpowsour.2005.03.160

Al electrode and a Li electrode. We also reported that the binder-free artificial graphite electrode [9] underwent the intercalation/deintercalation reaction of Li^+ and operated well as the negative electrode in the electrolyte melt [5]. Such a phenomenon is not seen with other ambient-temperature molten salts and ionic liquid salts.

In this study, we measured the physical properties of the LiCl-saturated $AlCl_3$–EMIC + $SOCl_2$ ($AlCl_3$–EMIC–$LiCl_{sat}$ + $SOCl_2$) melt, evaluated the possibility of the $AlCl_3$–EMIC–$LiCl_{sat}$ + $SOCl_2$ melt as a non-flammable electrolyte for the lithium secondary batteries and examined the electrode performance of the binder-free carbon-negative electrodes made by the electrophoretic deposition (EPD) method in the melt.

2. Experimental

EMIC was synthesized as previously reported [10]. The $AlCl_3$–EMIC melt was prepared by mixing EMIC with anhydrous $AlCl_3$ (Wako Pure Chemical Industries, Ltd.) at the predetermined molar ratio below 60 °C. The melt was purified by immersing Al wire into the melt for 1 week at room temperature [11]. Excessive anhydrous LiCl (Aldrich, 99.99%) was added to the melt. The LiCl-saturated melt was stirred at room temperature for 24 h, and a small quantity of $SOCl_2$ (Wako Pure Chemical Industries, Ltd.) was added to the melt and stirred for 6 h.

The density was measured by a Baume meter. The conductivity was measured by a conductivity meter (TOA Electronics, Ltd., CM-40S). The viscosity was measured by an Ostwald viscometer. The melting point was measured in the range of −115 to 25 °C by differential scanning calorimetry (Shimadzu Seisakusho, DSC-60).

The binder-free carbon-negative electrode was produced by the EPD method, so that various carbon materials of 1.8–2.0 mg cm^{-2} were deposited on Mo foil as previously reported [12].

The three-electrode cell consisted of a working electrode and a pressed Li foil on a Ni mesh current collector (R.E. and C.E.) was used for the electrochemical measurement. The electrochemical experiments were performed using a computer-controlled electrochemical measuring system (Hokuto Denko, HZ-3000) and an automatic battery charging-discharging instrument (Hokuto Denko, HJR-110mSM6). The scan rate of the cyclic voltammetry was 0.5 mV s^{-1}. The charge–discharge cycle tests were applied at 25 °C under the following conditions. The cells were discharged from their open circuit potential (OCP) to 0.0 V versus Li^+/Li and from OCP to 2.0 V versus Li^+/Li at a constant current density of 0.070 mA cm^{-2} (0.1 C). The cells were stored for 15 min, charged at a constant current density of 0.070 mA cm^{-2} (0.1 C) to 2.0 V versus Li^+/Li, and then stored for 15 min.

All procedures were carried out in an Ar atmosphere grove-box (MIWA MFG Co., Ltd., 1ADB–3LL).

Table 1
Some physical properties of 60.0 mol%$AlCl_3$–40.0 mol%EMIC–$LiCl_{sat}$ + $SOCl_2$ melt

Grass transition point (T_g) °C	−86.2
Density (mg cm^{-3}) (25 °C)	1.38
Viscosity (mPa s) (25 °C)	23.4
Conductivity (Ms cm^{-1}) (25 °C)	11.5
Electrochemical window (V)	4.2
V vs. Al(III)/Al	−2.0–2.2
Concentration of Li^+ (mol l^{-1})	1.6

3. Results and discussion

3.1. Physical properties of melt

The Lewis acidic melt (concentration of $AlCl_3$ in $AlCl_3$–EMIC melt > 50 mol%), which is liquid below room temperature and allows Li^+ to exist by adding LiCl, was used [4]. The physical properties of the 60.0 mol%$AlCl_3$–40.0 mol%EMIC–$LiCl_{sat}$ + 0.1 mol l^{-1} $SOCl_2$ melt are summarized in Table 1. Fig. 1 shows the DSC thermogram of the melt. No exothermic peak by cooling was observed and glass transition point (T_g) was observed at −86.2 °C. Therefore, the melt could be used as the electrolyte in a low-temperature domain. Although the density and the viscosity of the melt showed a slightly higher value than common organic solvent electrolytes, the conductivity was almost equal. When a cyclic voltammogram (C.V.) was measured with a W electrode, the electrochemical window was about 4.2 V. Moreover, as the reduction potential of the melt was ca. −2.2 V versus Al(III)/Al, it was clear that lithium can be deposited and stripped in this melt [4]. As mentioned above, the melt might be used as the electrolyte for non-flammable lithium secondary batteries.

3.2. Performance of binder-free carbon-negative electrode

Fig. 2 shows the relationship between the amount of the deposit and deposition voltage of the carbon materials.

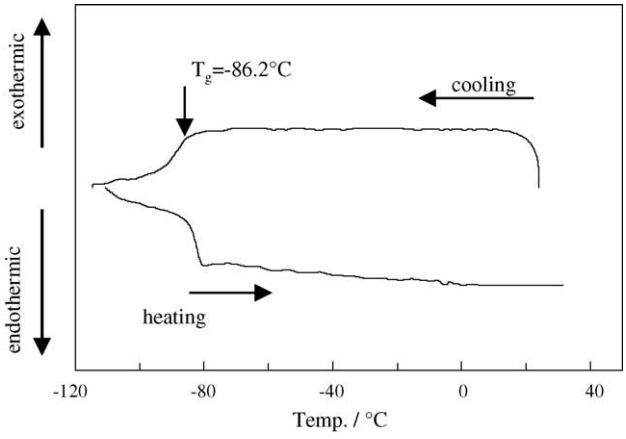

Fig. 1. DSC thermograms of 60.0 mol%$AlCl_3$–40.0 mol%EMIC–$LiCl_{sat}$ + $SOCl_2$ melt; heating and cooling rate, 10 K min^{-1}.

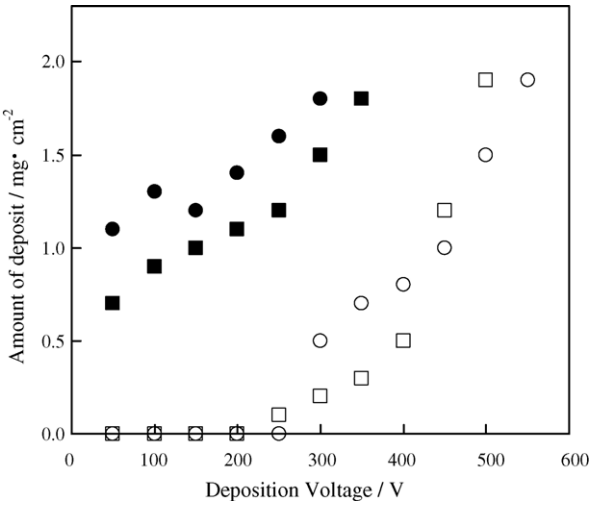

Fig. 2. Relationship between amount of deposit and deposition voltage (25 °C): (●) artifical graphite (KS-25); (■) natural graphite (LF-18A); (○) soft carbon (FM-14); (□) hard carbon (carbotron P).

The amount of the deposit increased, so that the deposition voltage was high for the artificial graphite (KS-25), natural graphite (LF-18A), soft carbon (FM14), and hard carbon (carbotron P). However, the mesocarbon microbeads powder was not able to be deposited. There was a slight amount of deposit of the soft carbon and hard carbon at deposition voltage equal to or less than 250 V, but it suddenly increased to higher than 250 V. The amount of the deposit, ca. 2.0 mg cm^{-2}, was obtained on the Mo current collector surface at the deposition voltage of the artificial graphite 300 V, natural graphite 350 V, soft carbon 550 V, and hard carbon 500 V, respectively. The surfaces of the binder-free carbon material film produced by the EPD method were observed (Fig. 3). The surface morphologies of the binder-free carbon material film were uniform and minute. In this way, the electrophoretic deposition was possible for the carbon materials with different particle shapes and grain sizes.

First, the possibility of binder-free carbon electrode as a negative electrode was examined. The C.V. of the binder-free natural graphite electrode in the melt was measured. In the potential region from 0 to 0.2 V versus Li^+/Li, three coupled redox peaks were observed. The electrochemical behavior in the potential region from 0 to 0.2 V versus Li^+/Li was very similar to the one observed in the organic solvent electrolyte with a graphite–Lithium intercalation anode composed of artificial graphite and a binder (polyvinylidene fluoride) [13]. It is well-known that the representative three coupled redox peaks, indicating the phase transitions between the Li^+ intercalation stages, were observed in the organic solvent containing Li salt. The first, second, and third stages were identified as a stage for the formation of the structures composed of $Li_{0.16}C_6$, $Li_{0.5}C_6$, and LiC_6, respectively. The reduction wave was considered to be the Li^+ intercalation reaction and the

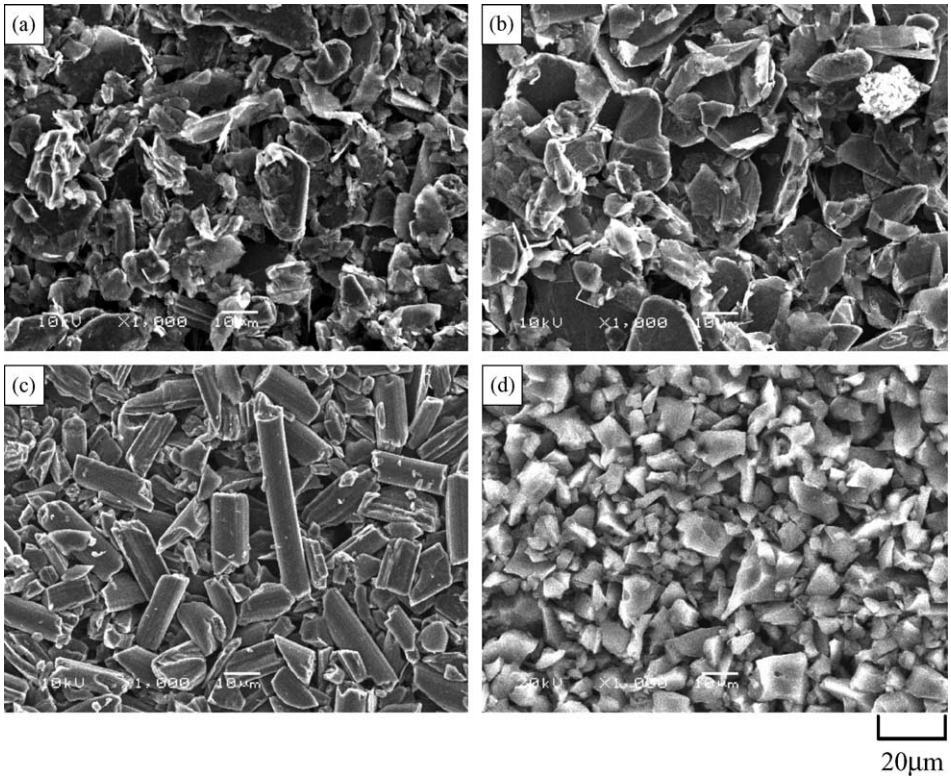

Fig. 3. SEM photographs of binder-free carbon films prepared by the electrophoretic deposition (EPD) method: (a) artifical graphite (KS-25); (b) natural graphite (LF-18A); (c) soft carbon (FM-14); (d) hard carbon (carbotron P).

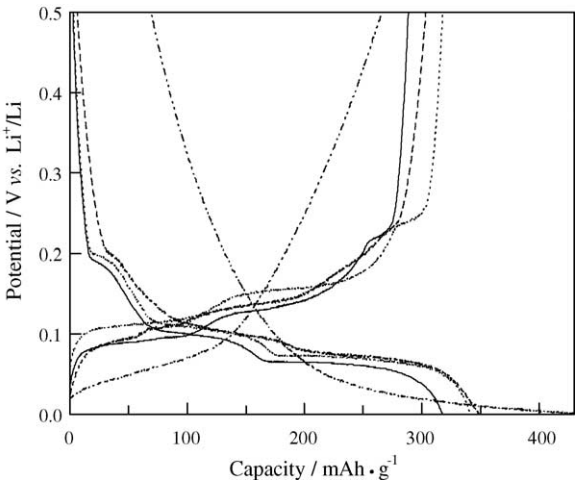

Fig. 4. Charge–discharge curves of the binder-free carbon electrodes at the 30th cycle (25 °C): C.D., 0.070 mA cm^{-2} (0.1 C); (—) artifical graphite (KS-25); (· · ·) natural graphite (LF-18A); (- - -) soft carbon (FM-14); (– · · –) hard carbon (carbotron P).

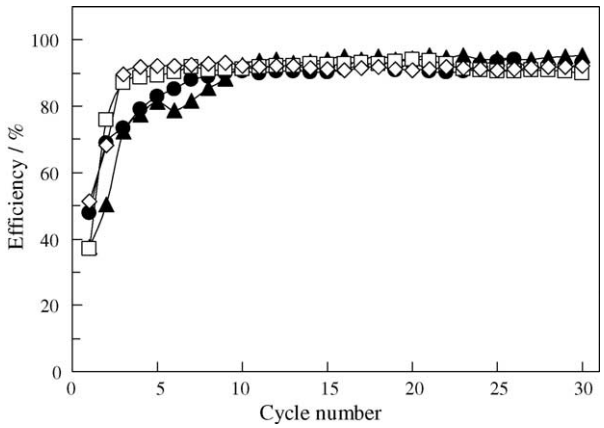

Fig. 5. Charge–discharge efficiencies of the binder-free carbon electrodes up to the 30th cycle (25 °C): C.D., 0.35 mA cm^{-2} (0.5 C) at first cycle, 0.070 mA cm^{-2} (0.1 C) at 2nd–30th cycles; (●) artifical graphite (KS-25); (▲) natural graphite (LF-18A); (□) soft carbon (FM-14); (◊) hard carbon (carbotron P).

oxidization wave was considered to be the Li^+ deintercalation reaction.

Next, the charge–discharge cycle tests of the binder-free carbon electrodes were performed. The charge–discharge curves of the binder-free carbon electrodes at the 30th cycle are shown in Fig. 4. These showed the same tendency as the charge–discharge curves of a carbon material in the organic solvent electrolyte. The discharge capacities of each carbon electrode at the 30th cycle were 296 mAh g^{-1} for artificial graphite, 325 mAh g^{-1} for natural graphite, 314 mAh g^{-1} for soft carbon, and 395 mAh g^{-1} for hard carbon, respectively. The charge–discharge efficiencies of the binder-free carbon electrodes are shown in Fig. 5. The charge–discharge efficiencies of the first cycle of all the carbon electrodes showed the low value of ca. 40–50%. The reason why the charge–discharge efficiencies of the first cycle are low may be due to the reduction of $SOCl_2$ and the formation of the surface electrolyte interphase (SEI) film accompanying it [8]. While the charge–discharge efficiencies of the artificial graphite and natural graphite reached 90% after the 10th cycle, the charge–discharge efficiencies of the soft carbon and hard carbon reached 90% in the third cycle. The charge–discharge efficiencies of each carbon electrode at the 30th cycle were 93.2% for artificial graphite, 95.3% for natural graphite, 90.0% for soft carbon, and 92.1% for hard carbon, respectively, so all the electrodes maintained 90% or better.

Finally, the surface of the binder-free natural graphite electrode before and after charging was observed (Fig. 6). The surface before charging (before Li^+ intercalation) was black and its surface after charging (after Li^+ intercalation) was a golden-yellow color that showed the formation of the first stage LiC_6 [14]. Moreover, since its surface after charging (after Li^+ deintercalation) returned to black as shown in Fig. 6(a), it became clear that the electrochemical intercalation and deintercalation reaction of Li^+ in the binder-free carbon electrode had occurred in a reversible manner

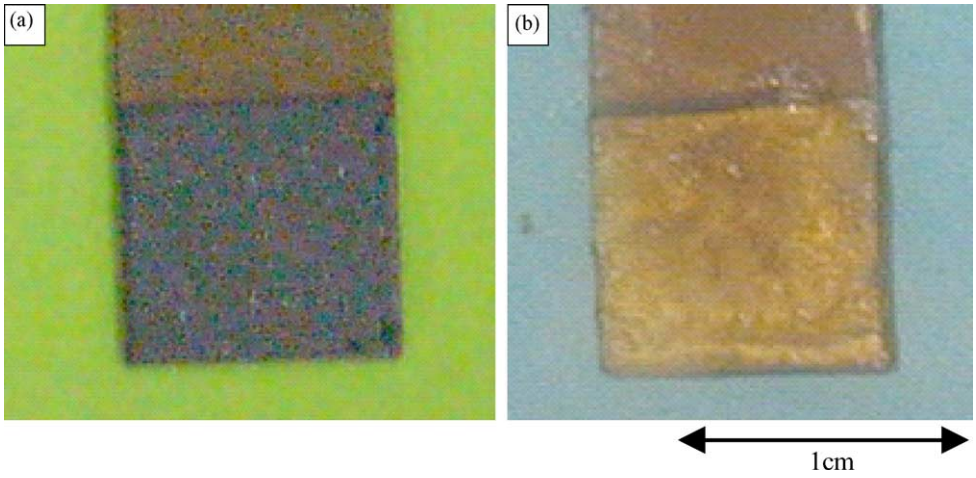

Fig. 6. Photographs of binder-free natural graphite electrode prepared by the EPD method: (a) before charging and (b) after charging (0 V vs. Li^+/Li).

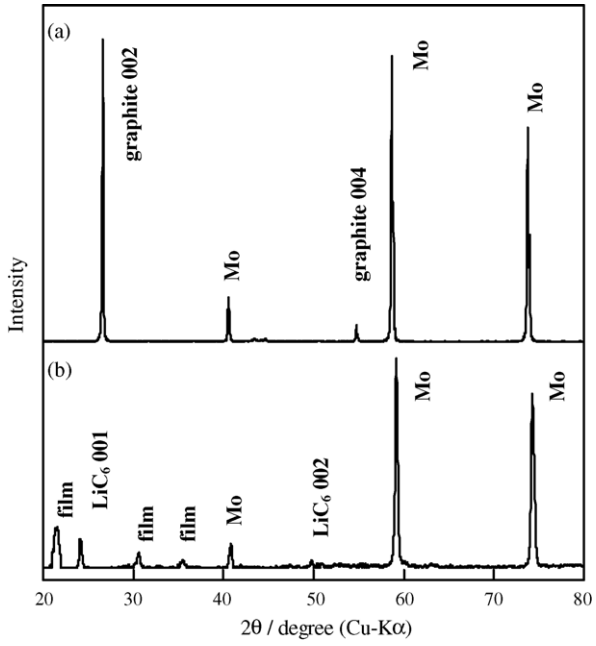

Fig. 7. XRD measurements of binder-free natural graphite electrode prepared by the EPD method: (a) before charging and (b) after charging (0 V vs. Li^+/Li).

in the ambient-temperature molten salt. An X-ray diffraction (XRD) measurement was then performed in order to investigate each stage's structural change in the binder-free natural graphite electrode before and after charging (Fig. 7). The diffraction peaks of the natural graphite, which belong to (0 0 2) plane observed at 26.6° and (0 0 4) plane observed at 54.7° before charging, were shifted to lower degrees of 24.1° and 49.3° correspond to (0 0 1) and (0 0 2), respectively, after charging. This indicates an increase in the distance between the graphite layers due to the Li^+ intercalation. Moreover, the average layer plane intervals calculated from a peak (24.1°and 49.3°) were 3.685 or 1.848 Å, respectively. These values support the stage LiC_6. The intercalation of Li^+ in natural graphite was proved in the melt.

Based on the above-mentioned results, the melt can be used as the electrolyte for non-flammable lithium secondary batteries and the binder-free carbon-negative electrode operates quiet effectively.

4. Conclusion

The performance of a binder-free carbon-negative electrode was investigated using the $AlCl_3$–EMIC–$LiCl_{sat}$ + $SOCl_2$ melt as the electrolyte for non-flammable lithium secondary batteries. Because the glass transition point of 60.0 mol%$AlCl_3$–40.0 mol%EMIC–$LiCl_{sat}$ + 0.1 mol l^{-1} $SOCl_2$ melt was −86.2 °C, the melt could be used as the electrolyte in a low-temperature domain. For 30 cycles, the discharge capacities of the binder-free carbon electrode made by the electrophoretic deposition method were 296–395 mAh g^{-1} and the charge–discharge efficiencies were greater than 90%. These results lead to the conclusion that the melt can be used as the electrolyte for non-flammable lithium secondary batteries and the binder-free carbon-negative electrode operates quite effectively.

Acknowledgements

This work was partially supported by a Grant-in-Aid for Young Scientist (B) from the Ministry of Education, Culture, Sports, Science and Technology, Japan (no. 15750158) and by the Society of Advanced Battery Technologies, Osaka Science and Technology Center (OSTEC) of Japan.

References

[1] K. Ui, N. Koura, Y. Idemoto, K. Iizuka, Denki Kagaku 65 (1997) 161 (presently Electrochemistry).
[2] N. Koura, K. Ui, Light Metals 47 (1997) 267.
[3] N. Koura, K. Ui, K. Takeishi, Light Metals 47 (1997) 273.
[4] N. Koura, K. Iizuka, Y. Idemoto, K. Ui, Electrochemistry 67 (1999) 706.
[5] N. Koura, K. Etoh, Y. Idemoto, F. Matsumoto, Chem. Lett. (2001) 1320.
[6] M. Lipsztain, R.A. Osteryoung, J. Electrochem. Soc. 132 (1985) 1126.
[7] C.S. Kelley, J. Fuller, R.T. Carlin, J.S. Wilkes, J. Electrochem. Soc. 139 (1992) 694.
[8] J. Fuller, R.A. Osteryoung, R.T. Carlin, J. Electrochem. Soc. 142 (1995) 3632.
[9] N. Koura, H. Tsuiki, N. Terakura, Y. Idemoto, F. Matsumoto, K. Ui, K. Yamada, T. Mitate, J. Surf. Finish. Soc. Jpn. 52 (2001) 143.
[10] J.S. Wilkes, J.A. Levisky, R.A. Wilson, C.L. Hussey, Inorg. Chem. 21 (1982) 1263.
[11] S. Takahashi, N. Koura, J. Electroanal. Chem. 188 (1985) 245.
[12] N. Koura, S. Funo, H. Tsuiki, Y. Idemoto, K. Ui, F. Matsumoto, J. Surf. Finish. Soc. Jpn. 53 (2002) 683.
[13] D. Aurbach, B. Markovsky, I. Weissman, E. Levi, Y. Ein-Eli, Electrochim. Acta 45 (1999) 67.
[14] Z. Jiang, M. Alamgir, K.M. Abraham, J. Electrochem. Soc. 142 (1995) 333.